Journal of Power Sources 196 (2011) 7195–7202

Contents lists available at ScienceDirect

Journal of Power Sources

journal homepage: www.elsevier.com/locate/jpowsour

Pressurized solid oxide fuel cells: Experimental studies and modeling

Stephanie Seidler[a,*], Moritz Henke[a], Josef Kallo[a], Wolfgang G. Bessler[a], Uwe Maier[b], K. Andreas Friedrich[a]

[a] German Aerospace Center (DLR), Pfaffenwaldring 38-40, D-70569 Stuttgart, Germany
[b] ElringKlinger AG, Max-Eyth-Straße 2, D-72581 Dettingen/Erms, Germany

ARTICLE INFO

Article history:
Received 15 July 2010
Received in revised form
23 September 2010
Accepted 29 September 2010
Available online 7 October 2010

Keywords:
Solid oxide fuel cell
Pressurization
SOFC
Hybrid power plant
Experiment
Modeling

ABSTRACT

The hybrid power plant project at DLR aims at investigating the fundamentals and requirements of a combined fuel cell and gas turbine power plant. A specific aim is to demonstrate stable operation of a plant in the 50 kW class. Prerequisite for the power plant realization is the detailed characterization of each subsystem and their interactions. The pressurized solid oxide fuel cell (SOFC) is an essential part of one main subsystem. A combined theoretical and experimental approach allows a thorough insight into nonlinear behavior. This paper focuses on the influence of pressurization on SOFC performance in the range from 1.4 to 3 bar. Conclusions are based on experimental $V(i)$-characteristics as well as on overpotentials derived from elementary kinetic models. Experiments are performed on planar, anode-supported 5-cell short stacks. The performance increases from 284 mW cm^{-2} at 1.4 bar to 307 mW cm^{-2} at 2 bar and 323 mW cm^{-2} at 3 bar (at 0.9 V; anode: H_2/N_2 1/1; cathode: air; temperature: 800 °C). The benefit of a temperature rise increases at elevated pressures. Moreover, the effect of gas variation is enhanced at higher pressures. The main conclusion is that pressurization improves the performance. Due to different effects interfering, operation of pressurized SOFC requires further detailed analysis.

1. Introduction

The international energy agency predicts an increase in the demand of electrical energy by 76% worldwide in the next two decades [1]. Hence, power plants with high electrical efficiency and low emissions are required. One way to reach this goal is the hybrid power plant, consisting of a pressurized solid oxide fuel cell (SOFC) system coupled with a gas turbine. In addition to high electrical efficiency (>60%), hybrid power plants have a wide range of applications (some 10 kW up to multi MW). As a first step to realize full-scale power plants the German Aerospace Center (DLR) has started a project which aims to demonstrate a hybrid power plant with stable operation in the 50 kW class. To achieve this goal, the DLR Institutes of Technical Thermodynamics and Combustion Technology cooperate, joining their expertise in fuel cell and gas turbine technology.

To design the hybrid system and its control, the knowledge of the characteristics of each component and their interactions is needed. One essential part is the pressurized SOFC. In the context of the hybrid power plant the fuel cells will be operated in a pressure range from 1 to 8 bar. The behavior of SOFC at elevated pressures needs to be regarded under two aspects. On the one hand the effect of elevated pressure on the electrochemical behavior has to be understood. On the other hand, on account of our system focus, the steady-state and transient operational behavior is an important research area. A combined theoretical and experimental approach is very valuable to gain a thorough understanding of pressurized SOFC.

The present work focuses on the characterization of SOFC short stacks at elevated operating pressure. Due to complex and interdependent mechanisms inside a SOFC the behavior at elevated pressures cannot be derived from measurements at ambient conditions. In addition, there is no sufficient literature data. Hence, a test rig for characterizing SOFC short stacks at pressures up to 8 bar was set up. This paper presents first results from these experiments. In order to support interpretation of the observed behavior, elementary kinetic models are used.

2. Background

The timeliness and relevance of the hybrid power plant is evident from the number of groups working in the field. The most advanced research in developing system models regarding architecture and dynamic behavior is performed at University of Genoa, National Fuel Cell Research Center, Lund University, Norwegian University of Science and Technology and German Aerospace Center (DLR). University of Genoa works on the development of control

* Corresponding author. Tel.: +49 711 6862 279; fax: +49 711 6862 322.
E-mail addresses: Stephanie.Seidler@dlr.de (S. Seidler), Uwe.Maier@elringklinger.de (U. Maier).

0378-7753/$ – see front matter © 2010 Elsevier B.V. All rights reserved.
doi:10.1016/j.jpowsour.2010.09.100

strategies and cycle layout [2]. National Fuel Cell Research Center tested the pressurized hybrid of Siemens and uses this knowledge to evaluate operating strategies for the combined cycle [3,4]. Lund University is concerned with the development of models for the hybrid system with a focus on turbo machinery [5]. Norwegian University of Science and Technology created a hybrid system model toolbox [6,7]. Recent work of the German Aerospace Center involves gas turbine and SOFC models including the most important balance of plant components to design the hybrid system and its control [8,9]. To date, very few SOFC/GT hybrid systems have been built. Siemens has demonstrated the feasibility with its pressurized 200 kW SOFC/GT hybrid system (PH220) [10]. Mitsubishi Heavy Industries has reported that their 200 kW class SOFC/GT hybrid system has 3000 cumulative hours of operation [11,12]. Korea Institute of Energy Research did short tests with a 30 kW hybrid system: 5 kW SOFC combined with 25 kW gas turbine [13].

Very few experimental studies on pressurized SOFC have been published so far. Recent data is by Zhou et al. (Chinese Academy of Sciences) who report about tests on anode-supported, tubular cells with an active cell area of 100 cm^2. They performed tests in the temperature range between 650 and 800 °C at 1, 2, 4 and 6 atm with hydrogen at fuel utilizations of 10–90% on the anode and air on the cathode. The maximum power density with hydrogen at a fuel utilization of 70% on the anode and air on the cathode increases at 650 °C from 135 mW cm^{-2} at 1 atm to 159 mW cm^{-2} at 6 atm. At 800 °C the power density increases from 266.7 mW cm^{-2} at 1 atm to 306 mW cm^{-2} at 6 atm [14]. First tests on pressurized cells and bundles were performed by Westinghouse (which later became part of Siemens Energy). In 1992 a test rig was built to characterize one to four cells of up to 200 cm length at up to 15 atm. The cathode-supported, tubular cells have been tested at 1–5 atm with hydrogen and natural gas on the anode and air on the cathode. The performance gain is approximately 10% [15]. Singhal adds that the cell output power at 1000 °C increases by 9% from 1 to 5 atm and by 6% from 5 to 15 atm [16]. Pressurized testing for a limited time was reported by Lim et al. (Korea Institute of Energy Research) with a 5 kW class anode-supported planar SOFC stack. The stack consists of 40 cells with an active area of 361 cm^2. The power with hydrogen (humidity 10%) on the anode and air on the cathode at 0.44 A cm^{-2} increases from 4.8 kW at ambient pressure to 5 kW at 2 bar. They saw a smaller increase in power gain when increasing the pressure to 3.5 atm [13]. Other experiments of cells/stacks at elevated pressures were performed by Rolls Royce, Mitsubishi and General Electric. As this is private funded industrial research no data has been published as far as we are aware of.

3. Methods and set-up

3.1. Experimental details

The pressurized SOFC test rig enables DLR to characterize SOFC short stacks at pressures up to 8 bar, see Figs. 1 and 2. Owing to a complex and precise pressure control the pressure differences between anode/cathode/surroundings can be controlled on demand to be as low as 10 mbar or up to 500 mbar. It is important to keep the pressure differences low for two reasons. First, pressure differences may lead to the destruction of the cell. Second, pressure differences may cause enhanced or declined electrochemical activity of the cell. To enable the precise pressure control the volume of the stack (~100 ml) is balanced by equalizing tanks (400 l each) at the anode and cathode outlet to match the oven volume (~400 l). The parameters (gas composition, temperature and load) are chosen to enable testing of different SOFC designs at all relevant operating conditions. A wide range of gases such as hydrogen, nitrogen, argon, methane, carbon monoxide and carbon dioxide

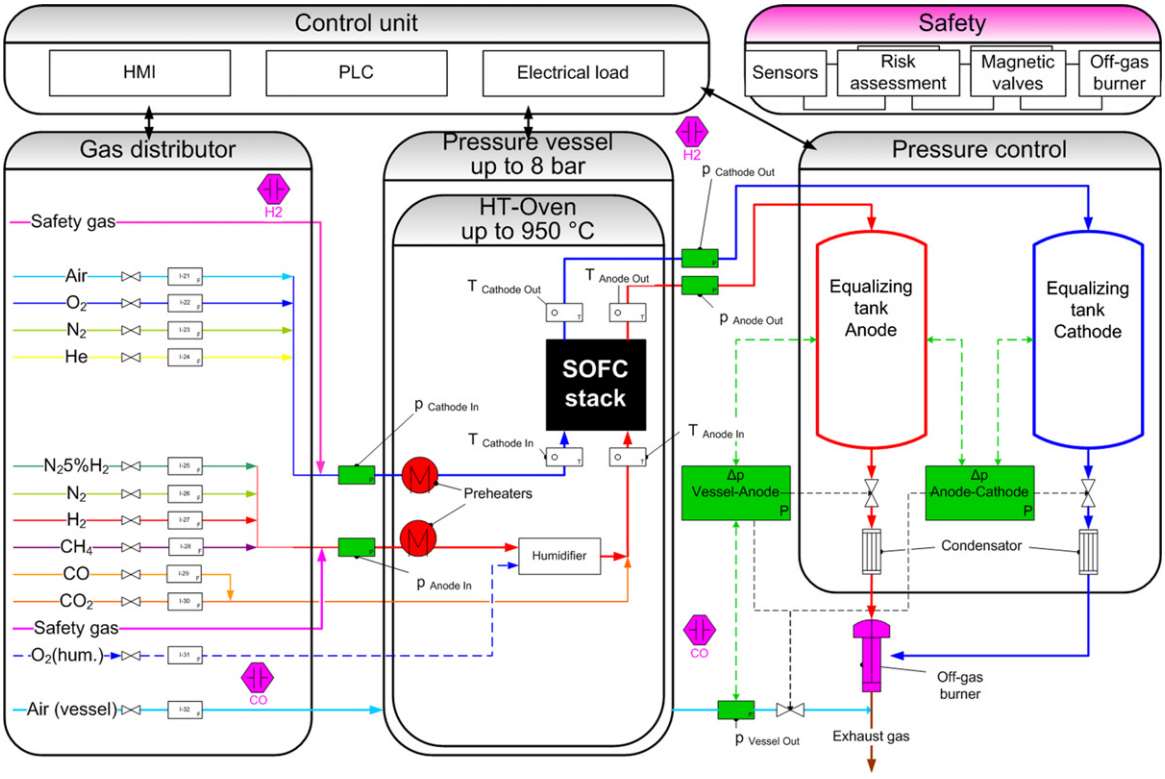

Fig. 1. Schematic of pressurized SOFC test rig. Left: Gases used for SOFC operation. Middle: SOFC stack with temperature and pressure sensors. Right: Equalizing tanks and pressure control. Top left: Control unit with human machine interface (HMI), programmable logic control (PLC) and electrical load. Top right: Safety measures (not described in detail), e.g. risk assessment, sensors, magnetic valves and off-gas burner.

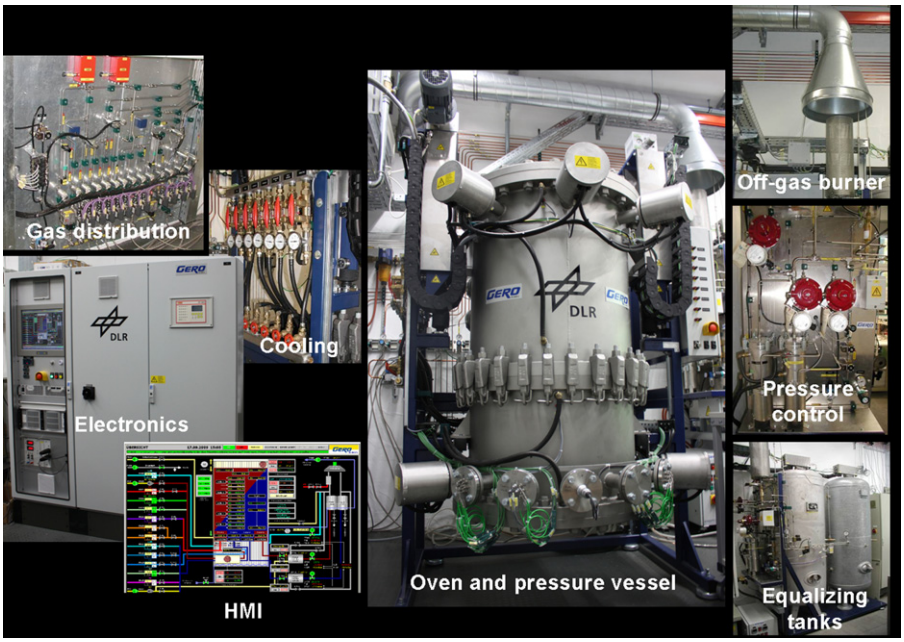

Fig. 2. Pressurized SOFC test rig: photographs of the most important parts.

with adjustable water vapor content up to 100% are available on the anode side and can be mixed to simulate reformate. Air, oxygen, nitrogen and helium or mixtures of these gases can be utilized on the cathode. The temperature of the cells can be adjusted up to 950 °C, the maximum temperature in the gas preheater is 800 °C. The cells/stack can be analyzed by $V(i)$-characteristics, impedance spectroscopy and gas analysis. The gas composition can be measured directly at anode and cathode in- and outlet. Special attention is paid to safety measures.

The examined SOFC are anode-supported 5-cell short stacks with an active area of 84 cm^2 $cell^{-1}$ provided by ElringKlinger AG. To build short stacks, sintered anode-supported cells (ASC) are integrated into cassettes consisting of two metal bipolar plates (CroFer22) which are laser welded. To form a stack the cassettes are welded between the gas module and the cathode contact sheet which is connected with to stack top plate. The anode consists of two layers made of Ni + YSZ: a 240 μm thick substrate and a 10 μm reactive layer. The next layer is a 10 μm YSZ electrolyte. The cathode again consists of two layers, a 10 μm reactive layer made of LSM + YSZ and a 60 μm current collector made of LSM, see Fig. 3.

In the experiments the pressure was adjusted at the anode cell outlet. The pressure differences between anode/cathode, anode/surroundings and cathode/surroundings were beneath 20 mbar at all times. Due to the nature of the test rig the minimum operating pressure is 1.4 bar. At each pressure the temperature was varied from 700 to 800 °C. The anode gas was changed in composition: pure hydrogen (H_2), hydrogen/nitrogen 1/1 (H_2/N_2 1/1) and hydrogen/nitrogen 3/1 (H_2/N_2 3/1). The total flow was set to 10 slpm for the whole 5-cell short stack. H_2/N_2 1/1 is used as an approximation of reformate gas. The cathode gas was air with a total flow of 15 slpm. For analysis $V(i)$-characteristics were used.

To begin with the correct operation of the test rig is verified by comparing measurements at ambient pressure with experimental in-house data [17]. Fig. 4 demonstrates the functionality of the test rig through the close similarity (deviation <2%) between measurements at ambient conditions with anode gas 5 slpm H_2 + 5 slpm N_2 + 4% H_2O (humidified hydrogen/nitrogen 1/1) at 750 °C on our test rig to in-house data with anode gas 5 slpm H_2 + 5 slpm N_2 + 3% H_2O at 750 °C and 21 slpm air on the cathode with the same stacks on another stack test rig.

3.2. Modeling

The theoretical research performed to support hybrid power plant development at DLR includes modeling and simulation on

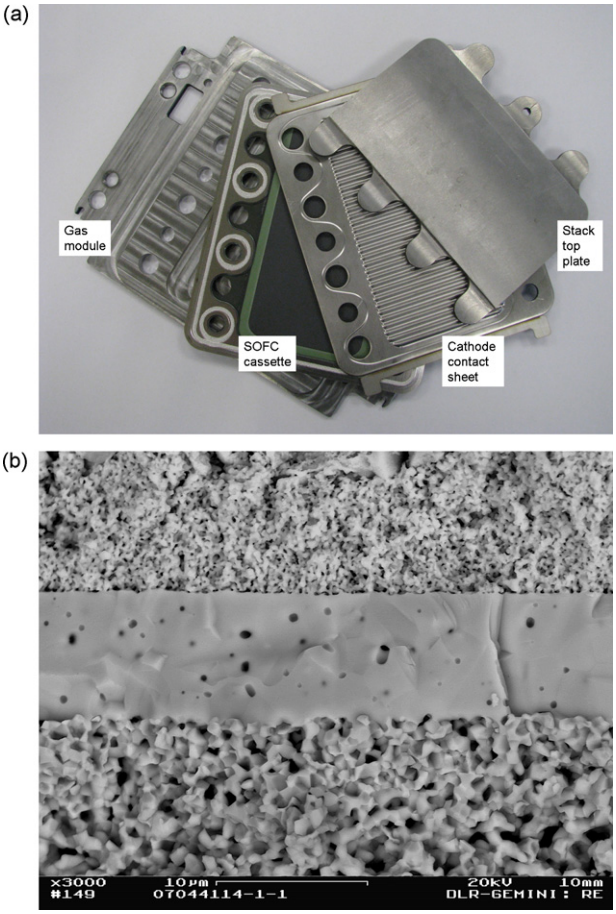

Fig. 3. (a) Stack components [17] and (b) cross section of an anode-supported cell imaged by SEM.

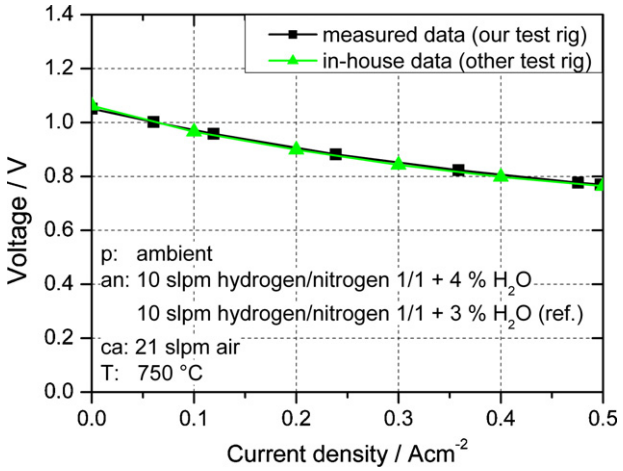

Fig. 4. Verification of test rig functionality: comparison of measured cell performance with previous experimental in-house data on the same stacks [17] (ambient pressure; an: 10 slpm H_2/N_2 1/1 +4% H_2O; ca: 21 slpm air; T: 750 °C).

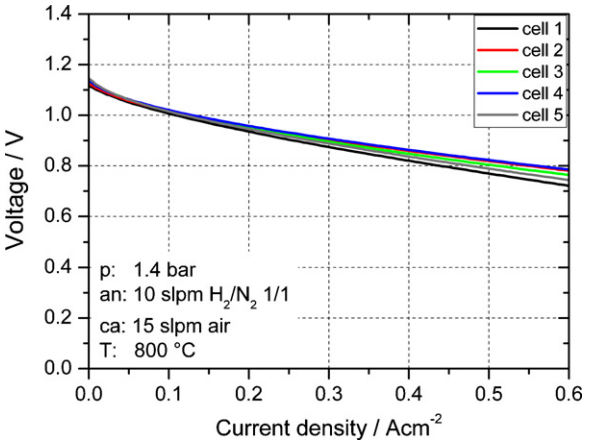

Fig. 5. Comparison of measured single-cell behavior in 5-cell short stack through $V(i)$-characteristics (p: 1.4 bar; an: H_2/N_2 1/1; ca: air; T: 800 °C).

cell and system level. This allows investigations that are difficult, expensive or time-consuming if conducted experimentally and provides insight into voltage loss contributions and optimization potentials.

For a detailed examination on the cell level an in-house software code is used [18]. The model is based on physical equations and is applicable to elevated pressures [19]. The results presented here are based on a model of anode-supported cells that was previously validated at ambient pressure [20]. Anode electrochemistry is described using elementary kinetics for surface reactions and charge transfer. Cathode electrochemistry is described via a Butler–Volmer equation. Even though the model does not exactly represent the experimentally examined cells, the current model provides sufficient accuracy as both cells are comparable (both anode supported and consisting of similar anode materials). It can be assumed that the pressure-dependent mechanisms are similar. A new cell model representing the experimentally examined cells will be developed and validated in the future.

Results shown in this work are from 2D simulations (dimensions are along the gas channels and through the thickness of the cell). All simulations are isothermal. The operation parameters of the simulations (pressure, temperature, gas composition) have been set according to the experiments. Fuel consists of hydrogen/nitrogen 1/1 or pure hydrogen respectively, with a humidity of 0.5%. Oxidant consists of 21% O_2 and 79% N_2. In analogy to the flows of the experimentally investigated cells (10 slpm stack^{-1} on the anode, 15 slpm stack^{-1} on the cathode), a fuel inlet flow of 0.024 slpm cm^{-2} and an oxidant inlet flow of 0.036 slpm cm^{-2} are chosen. On system level, the current work focuses on the dynamic behavior of a fuel cell system which is analyzed by step-response simulations as well as full load cycles. A control system of the power plant is implemented which can be optimized for different aspects, for example, heat conservation during low-load operation [8].

4. Results

In this paper the pressure-dependence of performance is investigated. To illustrate the effect of pressurization, temperature and gas composition on the anode are varied. The interdependencies of the mechanisms inside the SOFC are emphasized by combining two parameter changes. The focus is on the pressure range from 1.4 to 3 bar. Interpretation is derived from experiments ($V(i)$-characteristics) as well as from modeling/simulation results (overpotentials). For illustration purposes, all diagrams are based on cell 4 out of the 5-cell short stack. Cells 2, 3 and 4 show similar and consistent behavior. Owing to boundary effects, cells 1 and 5 differ in the absolute values but show qualitatively similar behavior (see Fig. 5).

4.1. Influence of elevated pressure on power density

To begin with, SOFC behavior at 1.4, 2 and 3 bar is illustrated in Fig. 6 through $V(i)$-characteristics and power density over current density plots at 800 °C with H_2/N_2 1/1 on the anode and air on the cathode. It can be seen that the open circuit voltage (OCV) increases with pressure rise according to Nernst potential. Namely, 1.136 V at 1.4 bar, 1.154 V at 2 bar and 1.189 V at 3 bar are measured. In addition, the power density increases at pressurization. At reference voltage of 0.9 V the power density is 284 mW cm^{-2} at 1.4 bar, 307 mW cm^{-2} at 2 bar and 323 mW cm^{-2} at 3 bar. This is an increase in performance of 8.3% from 1.4 to 2 bar and 13.8% from 1.4 to 3 bar. As expected from literature [14,15] the performance gain is comparatively higher from 1.4 to 2 bar than from 1.4 to 3 bar even though Zhou et al. compared 4 not 3 bar.

Further, it can be observed that performance gain (see Fig. 7) increases with voltage decrease or fuel utilization rise. For example, at a voltage of 1.0 V the performance gain is 18 mW cm^{-2} at 2 bar and 36 mW cm^{-2} at 3 bar. The performance gain increases at a voltage of 0.84 V to 30 mW cm^{-2} at 2 bar and 38 mW cm^{-2} at 3 bar. As high fuel utilizations are generally aimed for in SOFC systems, pressurization is bound to have a major effect on system level.

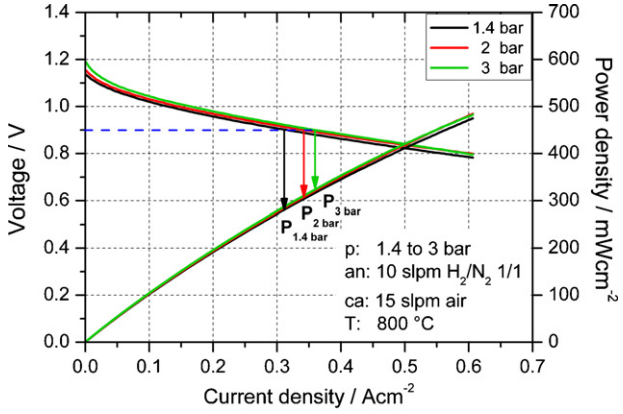

Fig. 6. Experimental $V(i)$-characteristics and power density over current density at 1.4, 2 and 3 bar (p: 1.4, 2 and 3 bar; an: H_2/N_2 1/1, ca: air, T: 800 °C).

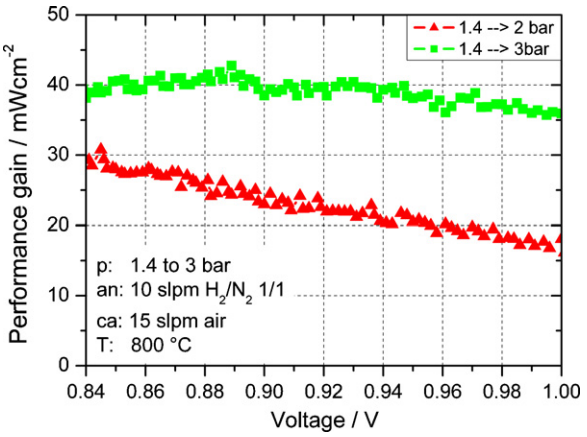

Fig. 7. Experimentally observed performance gain of 2 and 3 bar compared to 1.4 bar (an: H_2/N_2 1/1; ca: air, T: 800 °C).

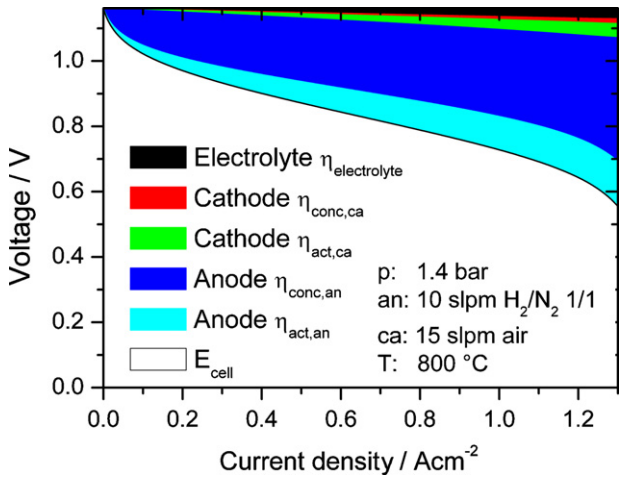

Fig. 9. Simulated overpotentials as a function of current density (p: 1.4 bar; an: H_2/N_2 1/1; ca: air; T: 800 °C).

4.2. Simulations and model-based analysis

Modeling and simulation are used to interpret experimental results. The simulated $V(i)$-characteristics of 1.4, 2 and 3 bar at 800 °C with hydrogen/nitrogen 1/1 on the anode and air on the cathode (displayed in Fig. 8) resemble the experimental data qualitatively. The performance of the simulated $V(i)$-characteristics is higher compared to the experimental observations which can be explained by model validation on different cells. However, the general behavior regarding pressure and temperature dependence is consistent. On this basis the model can be used for analysis of experimental results.

To determine the pressure-dependence of SOFC performance, the various losses in the cell can be expressed by overpotentials. From the physical model, three different types of overpotentials are derived: concentration, activation and ohmic losses (see Fig. 9). The activation overpotential includes adsorption/desorption, surface reactions and charge transfer based on the elementary kinetic description [18,20,21]. The concentration overpotential describes the resistance of molecules towards gas-phase transport. This includes diffusion through the electrodes as well as convective transport along the gas channels. Therefore, the concentration overpotential is strongly influenced by changes in species concentration (e.g. hydrogen concentration of the fuel gas) and electrode design (e.g. porosity). Furthermore activation and concentration overpotentials are influenced by operating conditions like temperature and pressure. The ohmic or electrolyte overpotential is a result of the limited ionic conductivity of the electrolyte. Other parts such as resistance of wires are not included at the present stage.

In Fig. 9 the characteristics of the overpotentials of an anode-supported cell at 1.4 bar and 800 °C are shown. The anodic overpotentials are dominant due to the thickness of the anode being ten times greater than the cathode thickness. All overpotentials but the electrolyte overpotential increase non-linearly as current density increases. Ohmic (electrolyte) losses increase linearly with increasing current density, as the ohmic overpotential is only dependent on current and temperature.

The pressure-dependence of the overpotentials simulated at 1 A cm^{-2} with hydrogen/nitrogen 1/1 on the anode and air on the cathode at 800 °C is shown in Fig. 10. When the pressure is increased from 1.4 to 3 bar concentration and activation overpotentials at both electrodes decrease. The concentration overpotential decreases because the concentration of hydrogen in the fuel and oxygen in the oxidant increases with increasing pressure because volume and temperature are constant. The concentration increase has a positive effect on diffusion through the electrodes. This leads to higher surface coverage of adsorbed intermediates [19]. The decrease of concentration overpotential at the cathode is low compared to the anode due to its lower thickness. The activation

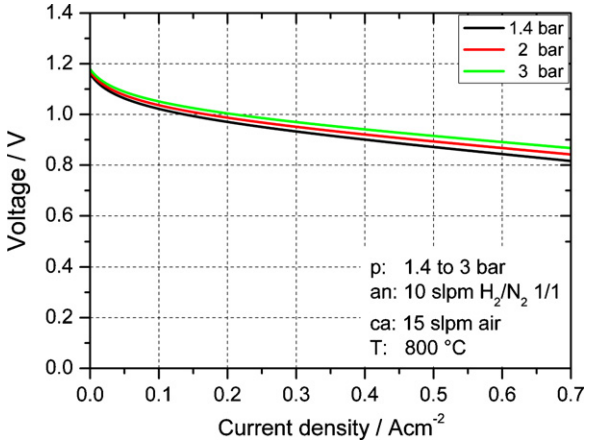

Fig. 8. Simulated $V(i)$-characteristics at 1.4, 2 and 3 bar (an: H_2/N_2 1/1; ca: air; T: 800 °C).

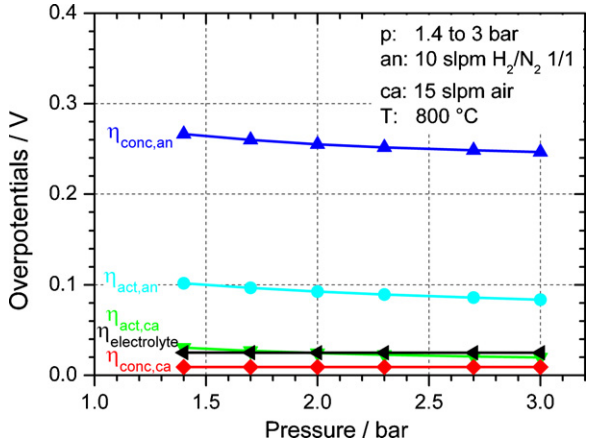

Fig. 10. Simulated overpotentials over pressure of 1.4–3 bar (1 A cm^{-2}; an: H_2/N_2 1/1; ca: air; T: 800 °C).

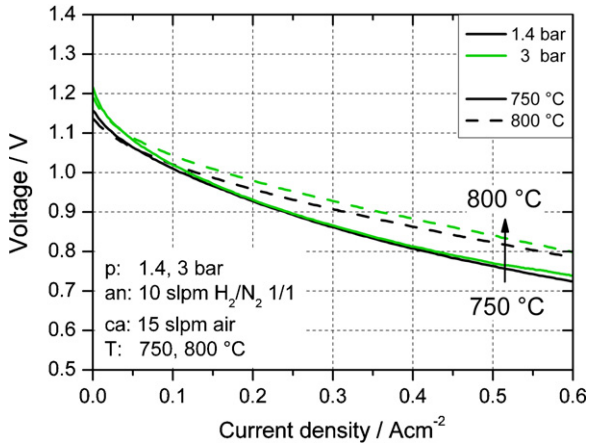

Fig. 11. Experimental $V(i)$-characteristics 1.4 and 3 bar at temperature variation from 750 to 800 °C (an: H_2/N_2 1/1; ca: air).

overpotentials decrease because the electron transfer steps, especially the hydrogen spillover at the anode surfaces, are favored at elevated pressures due to higher surface coverage with reacting species. As expected the electrolyte overpotential is not influenced by pressure.

4.3. Temperature variation at ambient pressure

To investigate the pressure-dependence of the different processes more closely the stack temperature and the gas composition on the anode were varied. Firstly, the effect of temperature variation was examined at ambient pressure. The experiments (Fig. 11) show that the temperature increase has a positive effect on the performance. The performance increase due to temperature rise from 750 to 800 °C at 1.4 bar is 30.9%.

Secondly, the simulated distribution of the overpotentials upon temperature rise (Fig. 12 at 1.4 bar) shows two interesting effects. On the one hand the temperature increase results in a decrease of activation overpotentials at the electrodes due to higher reaction rates. On the other hand, the concentration overpotentials increase slightly at temperature increase. This reflects the temperature dependence of the Nernst equation and has been shown before both theoretically [22] and experimentally [23]. Electrolyte overpotential decreases owing to enhanced ionic conductivity of the electrolyte.

4.4. Influence of elevated pressure on temperature variation

Analyzing experimental results of a temperature variation from 750 to 800 °C at 1.4 and 3 bar with H_2/N_2 1/1 on the anode and air on the cathode (illustrated in Fig. 11), it can be seen that temperature variation has a greater effect than pressure increase. For example the performance increase from 1.4 to 3 bar at 750 °C and 0.9 V is 2.3% contrasting to the performance increase due to temperature rise from 750 to 800 °C at 1.4 bar of 30.9%.

Moreover, modeling shows the same behavior. Fig. 12 illustrates the change in overpotentials over pressure at 750 and 800 °C according to modeling. The slopes of the activation overpotential at the anode and the cathode are lower. The concentration overpotential at the anode decreases with the same tendency at both temperatures. Pressure increase does not seem to have a major influence on temperature variation.

However, the benefit of the temperature rise can be increased by pressurization. For example the performance gain when changing temperature from 750 to 800 °C at 0.9 V increases from 45.6% at 3 bar to 30.9% at 1.4 bar with H_2/N_2 1/1 on the anode.

From this one could expect that by increasing both parameters (pressure and temperature) at the same time, the performance increase would be the sum of both effects. Experimentally the performance gain is even higher. The power density at 0.4 A cm^{-2} is 323 mW cm^{-2} at 1.4 bar and 750 °C. The benefit of the variation to 3 bar and 800 °C is +30 mW cm^{-2} (353 mW cm^{-2}). The sum of both effects would be +24 mW cm^{-2} (347 mW cm^{-2}). Interestingly, changing the conditions to pure hydrogen on the anode, similar trends are seen. The performance gain from 750 °C and 1.4 bar to 800 °C and 3 bar is also 30 mW cm^{-2} (341–372 mW cm^{-2}). This suggests that the gas change has no major influence on performance gains. This interpretation is supported by the same power density rise at different gas compositions on the anode and pressurization, in particular changing the operating conditions from 750 °C and 1.4 bar to 800 °C and 2 bar (H_2/N_2 1/1: +28 mW cm^{-2}, H_2: +27 mW cm^{-2}) as well as from 700 °C and 1.4 bar to 800 °C and 2 bar (H_2/N_2 1/1: +62 mW cm^{-2}, H_2: +63 mW cm^{-2}).

4.5. Gas variation at ambient pressure

The next variation is anode gas composition from H_2/N_2 1/1 to H_2/N_2 3/1 to pure H_2. At ambient conditions (as seen in Fig. 13, continuous lines) the measured power density at 0.9 V and 750 °C increases from 217 mW cm^{-2} with H_2/N_2 1/1 to 276 mW cm^{-2} with pure H_2 on the anode which is a gain of 27.5%.

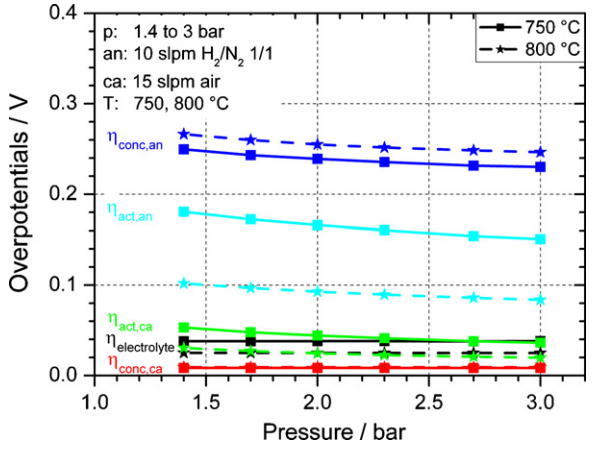

Fig. 12. Simulated overpotentials over pressure at 1.4–3 bar at temperature variation from 750 to 800 °C (at 1 A cm^{-2}; an: H_2/N_2 1/1; ca: air).

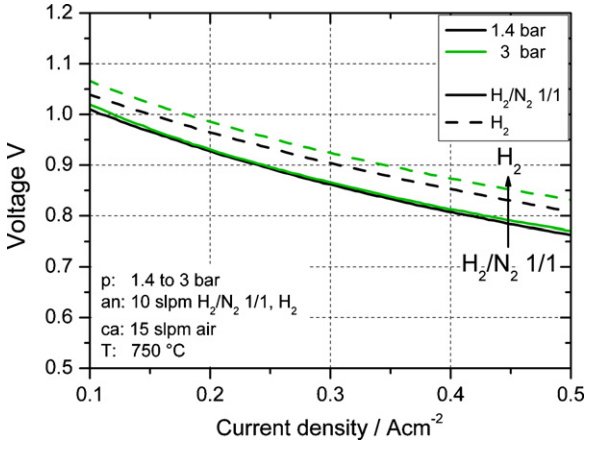

Fig. 13. Experimental $V(i)$-characteristics at 1.4 and 3 bar at gas variation from H_2/N_2 1/1 to H_2 (ca: air; T: 750 °C).

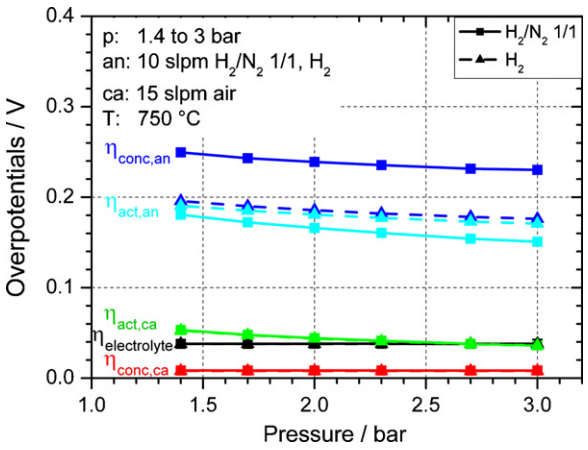

Fig. 14. Simulated overpotentials over pressure at 1.4–3 bar at gas variation from H_2/N_2 1/1 to H_2 (at 1 A cm^{-2}; ca: air; *T*: 750 °C).

Simulated changes in the overpotentials upon gas variation are shown in Fig. 14 (at 1.4 bar). The main effect is the decrease of concentration overpotential at the anode which is due to higher hydrogen concentration in the fuel and therefore results in improved availability of fuel gas in the porous electrodes. The activation overpotential at the anode increases slightly. This is due to the increasing H_2/H_2O ratio (note the constant humidification of 0.5% assumed in the model) which leads to decreased electrode kinetics [21,24]. Because the gas change is on the anode, the cathode overpotentials do not vary. The electrolyte overpotential is independent of gas composition at the electrodes.

4.6. Influence of elevated pressure on gas variation

Studying the gas variation from H_2/N_2 1/1 to pure H_2 at 1.4 and 3 bar at 750 °C (illustrated in Fig. 13), it can be seen that the performance gain of the gas change is greater than that of the pressure increase. For example the performance gain of gas change at 0.9 V from H_2/N_2 1/1 to pure H_2 at 750 °C is 27.5% at 1.4 bar contrasting to the 2.3% performance gain of pressure change from 1.4 to 3 bar at 750 °C with H_2/N_2 1/1 on the anode.

Yet, the performance gain of gas change increases at pressurization. The performance gain at 0.9 V from H_2/N_2 1/1 to pure H_2 at 750 °C at 3 bar is 40.3% (+89 mW cm^{-2}) contrasting to 27.5% (+60 mW cm^{-2}) at 1.4 bar. Fig. 14 shows the overpotentials over pressure at gas composition variation on the anode. It can be observed that the tendencies of the overpotentials do not change significantly with gas change.

Hence, it can be expected that by combining the increases in both hydrogen concentration and pressure, the benefits would add up. Interestingly, the benefit is even higher. For example the power density (at 0.4 A cm^{-2}, 750 °C) at 1.4 bar and H_2/N_2 1/1 is 323 mW cm^{-2} and increases to 349 mW cm^{-2} at 3 bar and H_2 which is a benefit of 26 mW cm^{-2} (sum of the effects: +20 mW cm^{-2}). Moreover, at 800 °C the variation of pressure and gas composition has the exact same absolute benefit (+26 mW cm^{-2}). At a change in pressure and gas composition the temperature does not seem to have a major influence.

5. Summary and conclusions

This paper presented a combined experimental and modeling study on the influence of pressurization on SOFC performance in the pressure range from 1.4 to 3 bar. Interpretations were based on experimental *V*(*i*)-characteristics as well as on overpotentials determined from modeling. The experiments were performed on planar, anode-supported 5-cell short stacks provided by ElringKlinger AG. Gas composition on the anode has been varied from H_2/N_2 1/1 over H_2/N_2 3/1 to pure H_2. Stack temperature was changed from 700 to 800 °C.

At the reference voltage of 0.9 V the performance was 284 mW cm^{-2} at 1.4 bar, 307 mW cm^{-2} at 2 bar and 323 mW cm^{-2} at 3 bar with H_2/N_2 1/1 on the anode and air on the cathode at 800 °C. As observed before [13,15], the performance gain from 1.4 to 2 bar was comparatively higher than from 1.4 to 3 bar. In the present study, 8.3% performance increase from 1.4 to 2 bar and 13.8% from 1.4 to 3 bar were obtained. In addition, the performance gain due to pressurization increased with decreasing voltage or increasing fuel utilization. As a high fuel utilization is generally aimed for in SOFC systems, pressurization is bound to have a major effect on the system level.

It was further observed that an increase in temperature has a larger benefit at higher pressure. Moreover, the effect of gas variation increased at pressurization. If one parameter (either temperature or gas composition on the anode) and the pressure were changed, the third parameter did not seem to have a major influence. For example, pressure increase from 1.4 to 3 bar and temperature rise from 750 to 800 °C had the same absolute benefit of 30 mW cm^{-2} both with H_2/N_2 1/1 or H_2 on the anode.

Overall, the study has shown that pressurization has several positive effects on performance. Those effects partially interfere with each other. This shows the need for further detailed analysis of pressurized SOFC operation.

In future experiments the electrochemical behavior will be further examined by means of gas analysis at anode and cathode inlet and outlet and impedance spectroscopy. The next step in studying the operational behavior will be identifying the operational limits. Modeling on cell level will focus on the development of a model of the examined cells.

Acknowledgements

This work was funded by German Aerospace Center (DLR). The authors thank Christian Hellwig for fruitful discussions.

References

[1] World Energy Outlook 2009 Fact Sheet, International Energy Agency, Paris, 2009.
[2] P. Costamagna, L. Magistri, A.F. Massardo, Journal of Power Sources 96 (2001) 352–368.
[3] F. Mueller, R. Gaynor, A.E. Auld, J. Brouwer, F. Jabbari, G.S. Samuelsen, Journal of Power Sources 176 (2008) 229–239.
[4] R. Roberts, J. Brouwer, F. Jabbari, T. Junker, H. Ghezel-Ayagh, Journal of Power Sources 161 (2006) 484–491.
[5] A. Selimovic, Modelling of Solid Oxide Fuel Cells Applied to the Analysis of Integrated Systems with Gas Turbines, Lund University, 2002.
[6] C. Stiller, NTNU, 2006.
[7] C. Stiller, B. Thorud, O. Bolland, ASME Turbo Expo, 2005.
[8] F. Leucht, W. Bessler, J. Kallo, K.A. Friedrich, 9th European SOFC Forum, Luzern, Switzerland, 2010.
[9] T. Panne, A. Widenhorn, M. Aigner, ASME Turbo Expo, 2008.
[10] S.E. Veyo, L.A. Shockling, J.T. Dederer, J.E. Gillet, W.L. Lundberg, Journal of Engineering for Gas Turbines and Power 124 (2002) 845–849.
[11] T. Gengo, Technical Review, Mitsubishi Heavy Industries, 2007, pp. 13–16.
[12] T. Gengo, Technical Review, Mitsubishi Heavy Industries, 2008, pp. 33–36.
[13] T.-H. Lim, R.-H. Song, D.-R. Shin, J.-I. Yang, H. Jung, I.C. Virke, S.-S. Yang, International Journal of Hydrogen Energy 33 (2008) 1076–1083.
[14] L. Zhou, M. Cheng, B. Yi, Y. Dong, Y. Cong, W. Yang, Electrochimica Acta 53 (2008) 5195–5198.
[15] E.R. Ray, R.A. Basel, J.F. Pierre, Fuel Cells '95 Review Meeting, Morgantown, United States, Westinghouse Electric Corporation, 1995.
[16] S.C. Singhal, Fifth International Symposium on Solid Oxide Fuel Cells, Aachen, Germany, 1997.
[17] M. Lang, T. Weckesser, C. Auer, P. Jentsch, K.A. Friedrich, C. Westner, ECS Transactions, Vienna, Austria, 2009.
[18] W.G. Bessler, S. Gewies, M. Vogler, Electrochimica Acta 53 (2007) 1782–1800.
[19] M. Henke, J. Kallo, K.A. Friedrich, W.G. Bessler, Fuel Cells, submitted for publication.

[20] W.G. Bessler, S. Gewies, C. Willich, G. Schiller, K.A. Friedrich, Fuel Cells 10 (3) (2009) 411–418.
[21] M. Vogler, A. Bieberle-Hütter, L.J. Gauckler, J. Warnatz, W.G. Bessler, Journal of the Electrochemical Society 156 (2009) B663–B672.
[22] W.G. Bessler, S. Gewies, Journal of the Electrochemical Society 154 (2007) B548–B559.
[23] S. Primdahl, M. Mogensen, Journal of the Electrochemical Society 145 (1998) 2431–2438.
[24] W.G. Bessler, M. Vogler, H. Störmer, D. Gerthsen, A. Utz, A. Weber, E. Ivers-Tiffée, Physical Chemistry Chemical Physics (2010), doi:10.1039/C0CP00541J.

Glossary

Δp: Pressure difference
Act: Activation
An: Anode
ASC: Anode-supported cell
Ca: Cathode
CH_4: Methane
CO: Carbon monoxide
CO_2: Carbon dioxide
Conc: Concentration
El: Electrolyte
GT: Gas turbine
H_2: Hydrogen
$H_2O(YSZ)$: Water adsorbed on YSZ
H(Ni): Hydrogen adsorbed on nickel
HMI: Human machine interface
HT: High temperature
i: Current density ($mA\,cm^{-2}$)
LSM: Lanthanum strontium manganite
N_2: Nitrogen
$N_2/5\%H_2$: Safety gas
Ni: Nickel
NiO: Nickeloxide
O_2: Oxygen
O(Ni): Oxygen adsorbed on nickel
$O^{2-}(YSZ)$: Oxygen ion adsorbed on YSZ
OCV: Open circuit voltage
$OH^-(YSZ)$: Hydroxide adsorbed on YSZ
p: Pressure (bar)
P: Power density ($mW\,cm^{-2}$)
PLC: Programmable logic control
PNG: Purified natural gas
PSOFC: Pressurized solid oxide fuel cell
slpm: standard liter per minute
SOFC: Solid oxide fuel cell
T: Temperature (°C)
YSZ: Yttrium stabilized zirconium oxide